Original Article | Thyroid

eISSN 2005-8330
https://doi.org/10.3348/kjr.2022.0079
Korean J Radiol 2022;23(7):763-772

Korean Journal of Radiology
KJR

Clinicoradiological Characteristics in the Differential Diagnosis of Follicular-Patterned Lesions of the Thyroid: A Multicenter Cohort Study

Jeong Hoon Lee[1], Eun Ju Ha[1], Da Hyun Lee[1], Miran Han[1], Jung Hyun Park[1], Ji-hoon Kim[2]

[1]Department of Radiology, Ajou University School of Medicine, Suwon, Korea; [2]Department of Radiology, Seoul National University Hospital, Seoul National University College of Medicine, Seoul, Korea

Objective: Preoperative differential diagnosis of follicular-patterned lesions is challenging. This multicenter cohort study investigated the clinicoradiological characteristics relevant to the differential diagnosis of such lesions.

Materials and Methods: From June to September 2015, 4787 thyroid nodules (≥ 1.0 cm) with a final diagnosis of benign follicular nodule (BN, n = 4461), follicular adenoma (FA, n = 136), follicular carcinoma (FC, n = 62), or follicular variant of papillary thyroid carcinoma (FVPTC, n = 128) collected from 26 institutions were analyzed. The clinicoradiological characteristics of the lesions were compared among the different histological types using multivariable logistic regression analyses. The relative importance of the characteristics that distinguished histological types was determined using a random forest algorithm.

Results: Compared to BN (as the control group), the distinguishing features of follicular-patterned neoplasms (FA, FC, and FVPTC) were patient's age (odds ratio [OR], 0.969 per 1-year increase), lesion diameter (OR, 1.054 per 1-mm increase), presence of solid composition (OR, 2.255), presence of hypoechogenicity (OR, 2.181), and presence of halo (OR, 1.761) (all $p < 0.05$). Compared to FA (as the control), FC differed with respect to lesion diameter (OR, 1.040 per 1-mm increase) and rim calcifications (OR, 17.054), while FVPTC differed with respect to patient age (OR, 0.966 per 1-year increase), lesion diameter (OR, 0.975 per 1-mm increase), macrocalcifications (OR, 3.647), and non-smooth margins (OR, 2.538) (all $p < 0.05$). The five important features for the differential diagnosis of follicular-patterned neoplasms (FA, FC, and FVPTC) from BN are maximal lesion diameter, composition, echogenicity, orientation, and patient's age. The most important features distinguishing FC and FVPTC from FA are rim calcifications and macrocalcifications, respectively.

Conclusion: Although follicular-patterned lesions have overlapping clinical and radiological features, the distinguishing features identified in our large clinical cohort may provide valuable information for preoperative distinction between them and decision-making regarding their management.

Keywords: *Thyroid nodules; Thyroid cancer; Follicular neoplasm; Ultrasonography; Machine learning*

INTRODUCTION

Thyroid nodules are common in clinical practice and are detected by ultrasonography (US) in 10%–67% of patients [1-3]. Because the risk of malignancy in thyroid nodules is primarily assessed by US, clinical guidelines recommend US-based management. Both the US features of a thyroid nodule and its size determine the need for fine-needle aspiration (FNA), with the obtained cytologic results further contributing to patient management [1-3].

However, for follicular-patterned lesions, mainly benign follicular nodules (hyperplastic/adenomatoid nodule, BN), follicular adenoma (FA), follicular carcinoma (FC), and follicular variants of papillary thyroid carcinoma (FVPTC), the cytological features overlap, such that in some cases, they cannot be accurately distinguished by FNA alone [4,5].

Received: February 10, 2022 **Revised:** April 20, 2022
Accepted: April 26, 2022
Corresponding author: Eun Ju Ha, MD, PhD, Department of Radiology, Ajou University School of Medicine, 206 World cup-ro, Yeongtong-gu, Suwon 16499, Korea.
• E-mail: radhej@naver.com

Diagnostic uncertainty exists in 15%–30% of aspirates, including the Bethesda System for Reporting Thyroid Cytology category atypia/follicular lesions of undetermined significance (AUS/FLUS) [4]. In such cases, the differential diagnosis of benign and malignant follicular-patterned lesions is a major clinical challenge [6-10].

Previous studies have examined the value of molecular testing and core-needle biopsy (CNB) in the differential diagnosis and surgical planning of follicular-patterned lesions [11,12]. However, these advanced methods are expensive and not widely available. Moreover, they do not resolve the problem of overlap. Consequently, repetitive FNAs or diagnostic surgeries are commonly performed to obtain a conclusive diagnosis [6,11]. The use of US in the differentiation between benign and malignant thyroid nodules has been evaluated, but the study populations have been small, and the studies have been conducted at a single hospital. Therefore, to aid in the differential diagnosis of follicular-patterned lesions, we investigated their clinicoradiological characteristics in this multicenter cohort.

MATERIALS AND METHODS

Patient data were obtained from the Thyroid Imaging Network of the Korea Registry [13,14]. The Institutional Review Boards (IRBs) of the 26 participating centers approved the collection of anonymized data from the registry for research purposes. This retrospective study was approved by the IRB of Ajou University Medical Center, which waived the need for informed consent for the use of data (IRB No. AJIRB-MED-MDB-21-689).

Study Population

The 4787 nodules (obtained from 3610 female and 711 male; mean age: 54.2 ± 12.2 years) included in this study had a final diagnosis of BN (n = 4461), FA (n = 136), FC (n = 62), and FVPTC (n = 128) and were collected from June to September 2015. All FA, FC, and FVPTC nodules were diagnosed based on histopathological results after surgery. BNs (n = 4461) were likewise diagnosed based on postoperative histopathological results (n = 258) as well as the results of two or more CNBs (n = 601) and one benign FNA or CNB result (n = 3602).

US Examination and Image Analysis

All US examinations were performed using a 10–12 MHz or 5–14 MHz linear probe. US images were retrospectively reviewed by one of 17 experienced radiologists with 8–22 years of experience in performing thyroid US. After a meeting aimed at achieving consensus regarding image interpretation, image review was conducted using an online program (AIM AiCRO; https://study.aim-aicro.com) in which the nodules were assessed according to US guidelines with respect to composition, echogenicity, echotexture, calcification, margin, orientation, spongiform appearance, and halo [1,13,14]. If various types of calcifications (micro-, macro-, or rim-calcifications) were present in a nodule, it was considered positive for each category. All reviewers were blinded to the FNA results and final diagnoses. Finally, the nodules were classified according to the Korean Thyroid Imaging Reporting and Data System (K-TIRADS) [1,13,14].

Statistical Analysis

The clinical characteristics of the patients and the grayscale US features of the nodules were compared between the groups using the χ^2 test or Fisher's exact test. Student's *t* test was used to compare quantitative variables. Differences in the clinicoradiological characteristics of the groups were analyzed using univariable and multivariable logistic regression analyses. Follicular-patterned lesions were classified as BN, FA, FC, or FVPTC. Follicular-patterned neoplasms included FA, FC, and FVPTC, while follicular-patterned malignancies included FC and FVPTC. The least absolute shrinkage and selection operator (LASSO) was applied to determine the variables that best allowed nodule classification and minimize the potential collinearity between the variables in the multivariable logistic regression analysis [15]. *p* values were calculated using the Wald test [16]; a $p < 0.05$ was considered statistically significant.

A random forest model was used to investigate the relative importance of the clinical and US variables, and the random forest quantile classifier was used to address imbalances between groups [17-19]. The number of trees was inferred by minimizing the misclassification rate of out-of-bag samples. The relative importance of a feature is assigned based on the G-mean, defined as the geometric mean of the true-negative and true-positive rates [20].

RESULTS

Table 1 summarizes the clinicoradiological characteristics according to the type of follicular-patterned lesion. The

https://doi.org/10.3348/kjr.2022.0079

Korean Journal of Radiology
KJR

sex distribution of patients did not differ between the groups (p = 0.057). Patients with BN (54.7 ± 12.1) were significantly older than patients with FA (51.0 ± 12.0), FC (48.9 ± 13.7), or FVPTC (48.0 ± 11.5) (all p < 0.001). There were significant differences among the groups in terms of nodule size, composition, echogenicity, echotexture, calcifications, margin, spongiform appearance, halo, and K-TIRADS category (all p < 0.05), except for orientation

Table 1. Clinicoradiological Characteristics according to the Type of Follicular-Patterned Lesion

Variables	Total				*P*
	BN (n = 4461)	FA (n = 136)	FC (n = 62)	FVPTC (n = 128)	
Age, years					< 0.001
Mean ± SD	54.7 ± 12.1	51.0 ± 12.0	48.9 ± 13.7	48.0 ± 11.5	
Range	19–76	20–76	22–73	21–79	
Sex					0.057
Female	3757 (84.2)	103 (75.7)	53 (85.5)	110 (85.9)	
Male	704 (15.8)	33 (24.3)	9 (14.5)	18 (14.1)	
Diameter, mm					< 0.001
Mean ± SD	20.8 ± 10.5	29.4 ± 14.9	34.5 ± 14.4	22.9 ± 12.9	
Range	10–100	10–90	10–75	10–71	
Composition					< 0.001
Solid	2107 (47.2)	76 (55.9)	39 (62.9)	93 (72.6)	
Partially cystic	2354 (52.8)	60 (44.1)	23 (37.1)	35 (27.4)	
Echogenicity					< 0.001
Hypoechogenicity	1231 (27.6)	53 (39.0)	30 (48.4)	60 (46.9)	
Iso-/hyper-echogenicity	3230 (72.4)	83 (61.0)	32 (51.6)	68 (53.1)	
Echotexture					< 0.001
Uniform	3480 (78.0)	97 (71.3)	39 (62.9)	87 (68.0)	
Mixed	981 (22.0)	39 (28.7)	23 (37.1)	41 (32.0)	
Calcifications*					< 0.001
None	3485 (78.1)	108 (79.4)	36 (58.1)	80 (62.5)	
Microcalcification	553 (12.4)	20 (14.7)	14 (22.6)	27 (21.1)	
Macrocalcification	433 (9.7)	9 (6.6)	7 (11.3)	26 (20.3)	
Rim calcification	133 (3.0)	3 (2.2)	11 (17.7)	7 (5.5)	
Margin					< 0.001
Smooth	3618 (81.1)	127 (93.4)	58 (93.6)	103 (80.5)	
Non-smooth	843 (18.9)	9 (6.6)	4 (6.5)	25 (19.5)	
Orientation					0.144
Parallel	4262 (95.5)	131 (96.3)	60 (96.8)	117 (91.4)	
Nonparallel	199 (4.5)	5 (3.7)	2 (3.2)	11 (8.6)	
Spongiform appearance					0.003
None	4287 (96.1)	131 (96.3)	62 (100.0)	127 (99.2)	
Presence	174 (3.9)	5 (3.7)	0 (0.0)	1 (0.8)	
Halo					< 0.001
None	2847 (63.8)	59 (43.4)	25 (40.3)	65 (50.8)	
Presence	1614 (36.2)	77 (56.6)	37 (59.7)	63 (49.2)	
K-TIRADS					< 0.001
Category 2	302 (6.8)	7 (5.1)	0 (0.0)	4 (3.1)	
Category 3	2789 (62.5)	75 (55.2)	28 (45.2)	56 (43.8)	
Category 4	1135 (25.4)	45 (33.1)	28 (45.2)	42 (32.8)	
Category 5	235 (5.3)	9 (6.6)	6 (9.6)	26 (20.3)	

Data in parentheses are the percentages. *If various types of calcifications were present in a nodule, they were considered as positive for each category. BN = benign follicular nodule, FA = follicular adenoma, FC = follicular carcinoma, FVPTC = follicular variant of papillary thyroid carcinoma, K-TIRADS = Korean Thyroid Imaging Reporting and Data System, SD = standard deviation

https://doi.org/10.3348/kjr.2022.0079

Table 2. Univariable and Multivariable Logistic Regression Analyses for Benign Follicular Nodule (As the Control Group) vs. Follicular-Patterned Neoplasms

Variables*	Control vs. Follicular-Patterned Neoplasms (n = 326)			Control vs. FA (n = 136)			Control vs. FC (n = 62)			Control vs. FVPTC (n = 128)		
	OR	95% CI	*P*	OR	95% CI	*P*	OR	95% CI	*P*	OR	95% CI	*P*
Univariable analysis												
Age per 1-year increase	0.966	0.957–0.975	< 0.001	0.975	0.961–0.989	< 0.001	0.962	0.943–0.982	< 0.001	0.958	0.944–0.972	< 0.001
Sex (female)	1.204	0.892–1.600	0.212	1.710	1.130–2.522	0.009	0.906	0.416–1.755	0.786	0.873	0.510–1.409	0.599
Diameter per 1-mm increase	1.044	1.036–1.053	< 0.001	1.051	1.039–1.063	< 0.001	1.069	1.053–1.085	< 0.001	1.016	1.001–1.031	0.031
Solid composition (partially cystic)	1.969	1.562–2.493	< 0.001	1.415	1.005–2.001	0.048	1.894	1.137–3.228	0.016	2.969	2.024–4.453	< 0.001
Hypoechogenicity (isoechogenicity)	2.050	1.630–2.575	< 0.001	1.675	1.174–2.372	0.004	2.460	1.483–4.070	< 0.001	2.315	1.623–3.295	< 0.001
Mixed echotexture (homogeneous)	1.639	1.280–2.085	< 0.001	1.426	0.967–2.065	0.066	2.092	1.226–3.490	0.005	1.672	1.135–2.423	0.008
Calcification												
Microcalcification (absence)	1.627	1.205–2.164	0.001	1.218	0.731–1.929	0.423	2.061	1.088–3.662	0.019	1.889	1.202–2.872	0.004
Macrocalcification (absence)	1.372	0.966–1.905	0.067	0.658	0.308–1.230	0.229	1.181	0.488–2.439	0.681	2.365	1.491–3.622	< 0.001
Rim calcification (absence)	2.241	1.357–3.524	< 0.001	0.734	0.179–1.972	0.601	7.019	3.405–13.278	< 0.001	1.882	0.784–3.829	0.113
Non-smooth margin (smooth)	0.566	0.395–0.790	0.001	0.304	0.143–0.567	0.001	0.296	0.090–0.722	0.019	1.042	0.655–1.596	0.857
Non-parallel orientation (parallel)	1.252	0.737–1.999	0.375	0.817	0.287–1.822	0.662	0.714	0.117–2.305	0.641	2.014	1.009–3.632	0.031
Spongiform appearance (absence)	0.462	0.181–0.962	0.065	0.940	0.330–2.100	0.894	0.000	0.000–306.798	0.977	0.194	0.011–0.874	0.103
Halo (absence)	2.096	1.672–2.630	< 0.001	2.302	1.634–3.260	< 0.001	2.611	1.575–4.400	< 0.001	1.710	1.201–2.432	0.003
K-TIRADS												
K-TIRADS category 4 (category 3)	1.842	1.437–2.353	< 0.001	1.495	1.025–2.152	0.033	2.723	1.601–4.632	< 0.001	1.906	1.270–2.835	0.002
K-TIRADS category 5 (category 3)	3.172	2.176–4.532	< 0.001	1.444	0.668–2.758	0.305	2.818	1.046–6.427	0.023	5.700	3.479–9.102	< 0.001
Multivariable analysis												
Age per 1-year increase	0.969	0.959–0.978	< 0.001	0.979	0.966–0.993	0.003	0.969	0.948–0.989	0.003	0.955	0.941–0.970	< 0.001
Sex (female)	1.204	0.876–1.632	0.242	1.676	1.089–2.517	0.015	0.784	0.342–1.606	0.533	0.925	0.533–1.518	0.770
Diameter per 1-mm increase	1.054	1.044–1.064	< 0.001	1.058	1.045–1.071	< 0.001	1.084	1.065–1.103	< 0.001	1.026	1.010–1.042	0.001
Solid composition (partially cystic)	2.255	1.728–2.957	< 0.001	1.864	1.267–2.758	0.002	2.522	1.405–4.644	0.002	2.671	1.754–4.148	< 0.001
Hypoechogenicity (isoechogenicity)	2.181	1.681–2.828	< 0.001	2.102	1.416–3.104	< 0.001	2.785	1.569–4.956	< 0.001	1.936	1.314–2.848	< 0.001
Mixed echotexture (homogeneous)	1.201	0.921–1.556	0.170	1.056	0.699–1.564	0.792	1.421	0.794–2.485	0.225	1.297	0.868–1.906	0.194
Calcification												
Microcalcification (absence)	1.520	1.102–2.068	0.009	1.328	0.780–2.157	0.273	1.878	0.943–3.527	0.059	1.617	1.009–2.511	0.038
Macrocalcification (absence)	1.208	0.831–1.720	0.307	0.604	0.275–1.168	0.167	0.736	0.276–1.671	0.499	1.987	1.228–3.115	0.004
Rim calcification (absence)	1.762	1.032–2.878	0.030	0.646	0.155–1.806	0.472	6.005	2.639–12.751	< 0.001	1.355	0.554–2.828	0.459
Non-smooth margin (smooth)	0.691	0.468–0.995	0.054	0.406	0.186–0.784	0.013	0.359	0.102–0.961	0.067	1.077	0.653–1.724	0.764
Non-parallel orientation (parallel)	1.213	0.693–2.010	0.476	0.822	0.281–1.914	0.683	0.725	0.112–2.587	0.674	1.603	0.777–3.019	0.169
Halo (absence)	1.761	1.368–2.271	< 0.001	1.793	1.237–2.612	0.002	1.965	1.118–3.506	0.020	1.627	1.101–2.407	0.014

*The reference categories for OR calculations are in the parentheses. CI = confidence interval, FA = follicular adenoma, FC = follicular carcinoma, FVPTC = follicular variant of papillary thyroid carcinoma, K-TIRADS = Korean Thyroid Imaging Reporting and Data System, OR = odds ratio

https://doi.org/10.3348/kjr.2022.0079

Table 3. Univariable and Multivariable Logistic Regression Analyses for FA (As the Control Group) vs. Follicular-Patterned Malignancy

Variables*	Control vs. Follicular-Patterned Malignancy (n = 190)			Control vs. FC (n = 62)			Control vs. FVPTC (n = 128)		
	OR	95% CI	*P*	OR	95% CI	*P*	OR	95% CI	*P*
Univariable analysis									
Age per 1-year increase	0.983	0.965–1.001	0.072	0.987	0.963–1.011	0.276	0.981	0.961–1.001	0.070
Sex (female)	0.517	0.292–0.908	0.022	0.530	0.224–1.149	0.124	0.511	0.266–0.953	0.038
Diameter per 1-mm increase	0.987	0.972–1.002	0.095	1.023	1.002–1.044	0.029	0.966	0.947–0.984	< 0.001
Solid composition (partially cystic)	1.797	1.137–2.847	0.012	1.339	0.727–2.503	0.354	2.098	1.259–3.535	0.005
Hypoechogenicity (isoechogenicity)	1.409	0.903–2.210	0.132	1.468	0.800–2.696	0.214	1.382	0.848–2.259	0.195
Mixed echotexture (homogeneous)	1.263	0.786–2.048	0.338	1.467	0.772–2.763	0.237	1.172	0.693–1.986	0.554
Calcification									
Microcalcifications (absence)	1.596	0.897–2.918	0.119	1.692	0.778–3.605	0.176	1.551	0.823–2.961	0.177
Macrocalcification (absence)	2.966	1.423–6.800	0.006	1.796	0.614–5.064	0.269	3.597	1.669–8.440	0.002
Rim calcification (absence)	4.639	1.531–20.100	0.016	9.562	2.851–43.554	< 0.001	2.565	0.696–12.103	0.179
Non-smooth margin (smooth)	2.542	1.205–5.873	0.020	0.973	0.255–3.122	0.965	3.425	1.582–8.059	0.003
Non-parallel orientation (parallel)	1.924	0.707–6.119	0.224	0.873	0.123–4.179	0.874	2.463	0.869–8.009	0.104
Spongiform appearance (absence)	0.139	0.007–0.872	0.073	0.000	NA - 3.250E + 41	0.988	0.206	0.011–1.302	0.152
Halo (absence)	0.851	0.546–1.325	0.476	1.134	0.618–2.102	0.686	0.743	0.456–1.205	0.229
K-TIRADS									
K-TIRADS category 4 (category 3)	1.449	0.899–2.352	0.130	1.822	0.963–3.461	0.065	1.276	0.746–2.184	0.374
K-TIRADS category 5 (category 3)	3.313	1.546–7.762	0.003	1.952	0.608–5.915	0.241	3.948	1.781–9.485	0.001
Multivariable analysis									
Age per 1-year increase	0.976	0.957–0.996	0.018	0.993	0.966–1.020	0.588	0.966	0.943–0.989	0.004
Sex (female)	0.538	0.291–0.987	0.046	0.491	0.187–1.178	0.127	0.581	0.283–1.163	0.130
Diameter per 1-mm increase	0.997	0.979–1.015	0.722	1.040	1.014–1.068	0.003	0.975	0.953–0.996	0.024
Solid composition (partially cystic)	1.262	0.712–2.235	0.424	1.443	0.640–3.345	0.382	1.314	0.685–2.526	0.410
Hypoechogenicity (isoechogenicity)	1.213	0.711–2.074	0.478	1.589	0.745–3.416	0.232	1.037	0.562–1.907	0.906
Mixed echotexture (homogeneous)	1.436	0.857–2.425	0.172	1.728	0.841–3.548	0.135	1.315	0.727–2.391	0.365
Calcification									
Microcalcifications (absence)	1.196	0.625–2.329	0.592	1.567	0.641–3.781	0.318	1.020	0.474–2.187	0.959
Macrocalcification (absence)	2.930	1.323–7.069	0.011	1.801	0.499–6.368	0.359	3.647	1.559–9.242	0.004
Rim calcification (absence)	5.228	1.636–23.444	0.012	17.054	4.441–86.635	< 0.001	2.740	0.656–14.224	0.185
Non-smooth margin (smooth)	1.959	0.853–4.833	0.125	0.795	0.162–3.325	0.761	2.538	1.061–6.472	0.042
Non-parallel orientation (parallel)	1.421	0.449–5.047	0.563	0.859	0.084–5.811	0.885	1.551	0.455–5.838	0.493
Halo (absence)	1.003	0.604–1.663	0.992	1.245	0.588–2.675	0.569	1.019	0.578–1.803	0.949

*The reference categories for OR calculations are in the parentheses. CI = confidence interval, FA = follicular adenoma, FC = follicular carcinoma, FVPTC = follicular variant of papillary thyroid carcinoma, K-TIRADS = Korean Thyroid Imaging Reporting and Data System, NA = not applicable, OR = odds ratio

https://doi.org/10.3348/kjr.2022.0079

Korean Journal of Radiology KJR

(p = 0.144).

Distinction between BN and Follicular-Patterned Neoplasms (FA, FC, and FVPTC)

Table 2 shows the results of univariable and multivariable logistic regression analyses comparing BN and follicular-patterned neoplasms (FA, FC, and FVPTC). With BN as the control group, multivariable logistic regression analysis after LASSO regularization for feature selection showed that patient age (odds ratio [OR], 0.969 per 1-year increase; 95% confidence interval [CI], 0.959–0.978), maximal tumor diameter (OR, 1.054 per 1-mm increase; 95% CI, 1.044–1.064), presence of solid composition (OR, 2.255; 95% CI, 1.728–2.957), presence of hypoechogenicity (OR, 2.181; 95% CI, 1.681–2.828), and presence of halo (OR, 1.761; 95% CI, 1.368–2.271) were significant predictors of follicular-patterned neoplasms from BNs. Regarding calcifications, the presence of microcalcifications (OR, 1.617; 95% CI, 1.009–2.511) and macrocalcifications (OR, 1.987; 95% CI, 1.228–3.115) were significant for differentiating FVPTC from BN, and the presence of rim calcifications (OR, 6.005; 95% CI, 2.639–12.751) was significant for differentiating FC from BN.

Distinction between FA and Follicular-Patterned Malignancy (FC and FVPTC)

Table 3 shows the results of the univariable and multivariable logistic regression analyses comparing FA and follicular-patterned malignancy (FC and FVPTC). With FA as the control group, multivariable logistic regression analysis after LASSO regularization for feature selection showed that maximal tumor diameter (OR, 1.040 per 1-mm increase; 95% CI, 1.014–1.068) and rim calcifications (OR, 17.054; 95% CI, 4.441–86.635) were significant factors for differentiating FC from FA, whereas patient age (OR, 0.966 per 1-year increase; 95% CI, 0.943–0.989), maximal tumor diameter (OR, 0.975 per 1-mm increase; 95% CI, 0.953–0.996), macrocalcifications (OR, 3.647; 95% CI, 1.559–9.242), and non-smooth margins (OR, 2.538; 95% CI, 1.061–6.472) were significant factors for differentiating FVPTC from FA.

Distinction between BN/FA and Follicular-Patterned Malignancy (FC and FVPTC)

Supplementary Table 1 shows the results of the univariable and multivariable logistic regression analyses for BN/FA vs. follicular-patterned malignancies. With BN/FA as the control group, multivariable logistic regression analysis after LASSO regularization for feature selection showed that patient age (OR, 0.961 per 1-year increase; 95% CI, 0.949–0.973), maximal tumor diameter (OR, 1.045 per 1-mm increase; 95% CI, 1.033–1.057), solid composition (OR, 2.558; 95% CI, 1.809–3.657), hypoechogenicity (OR, 2.120; 95% CI, 1.530–2.936), and presence of a halo (OR, 1.701; 95% CI, 1.230–2.359) were significant for differentiating follicular-patterned malignancies from BNs/FAs. Regarding calcifications, rim calcifications (OR, 6.437; 95% CI, 2.853–13.572) were significant for differentiating FC from BN/FA, and microcalcifications (OR, 1.600; 95% CI, 0.999–2.485) and macrocalcifications (OR, 2.074; 95% CI, 1.283–3.248) were significant for differentiating FVPTC from BN/FA.

Relative Feature Importance by Random Forest Analysis

Figures 1 and 2 show the measures of relative importance for all the variables according to the random forest analysis. Maximal tumor diameter, solid composition, hypoechogenicity, non-parallel orientation, and age were the top five variables for differentiating follicular-patterned tumors (FA, FC, and FVPTC) from BNs. Rim calcification, microcalcification, maximal tumor diameter, age, and mixed

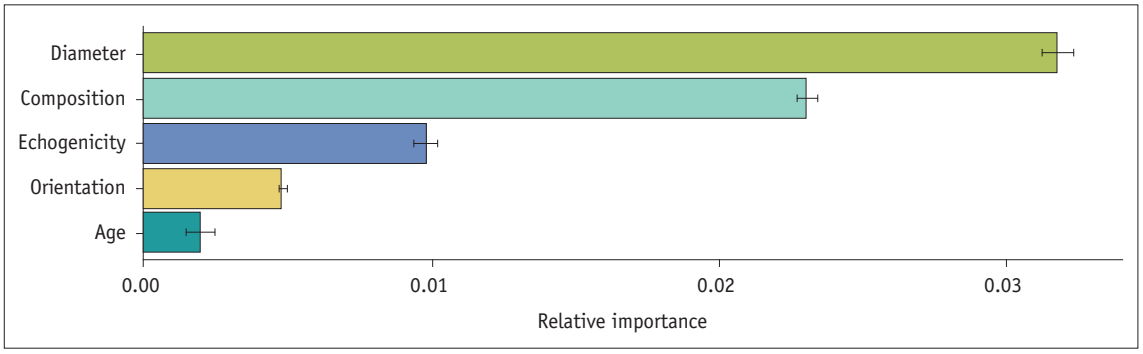

Fig. 1. The top five features important for distinguishing follicular-patterned neoplasms (follicular adenoma, follicular carcinoma, and follicular variant of papillary thyroid carcinoma) from benign follicular nodule.

https://doi.org/10.3348/kjr.2022.0079

Korean Journal of Radiology
KJR

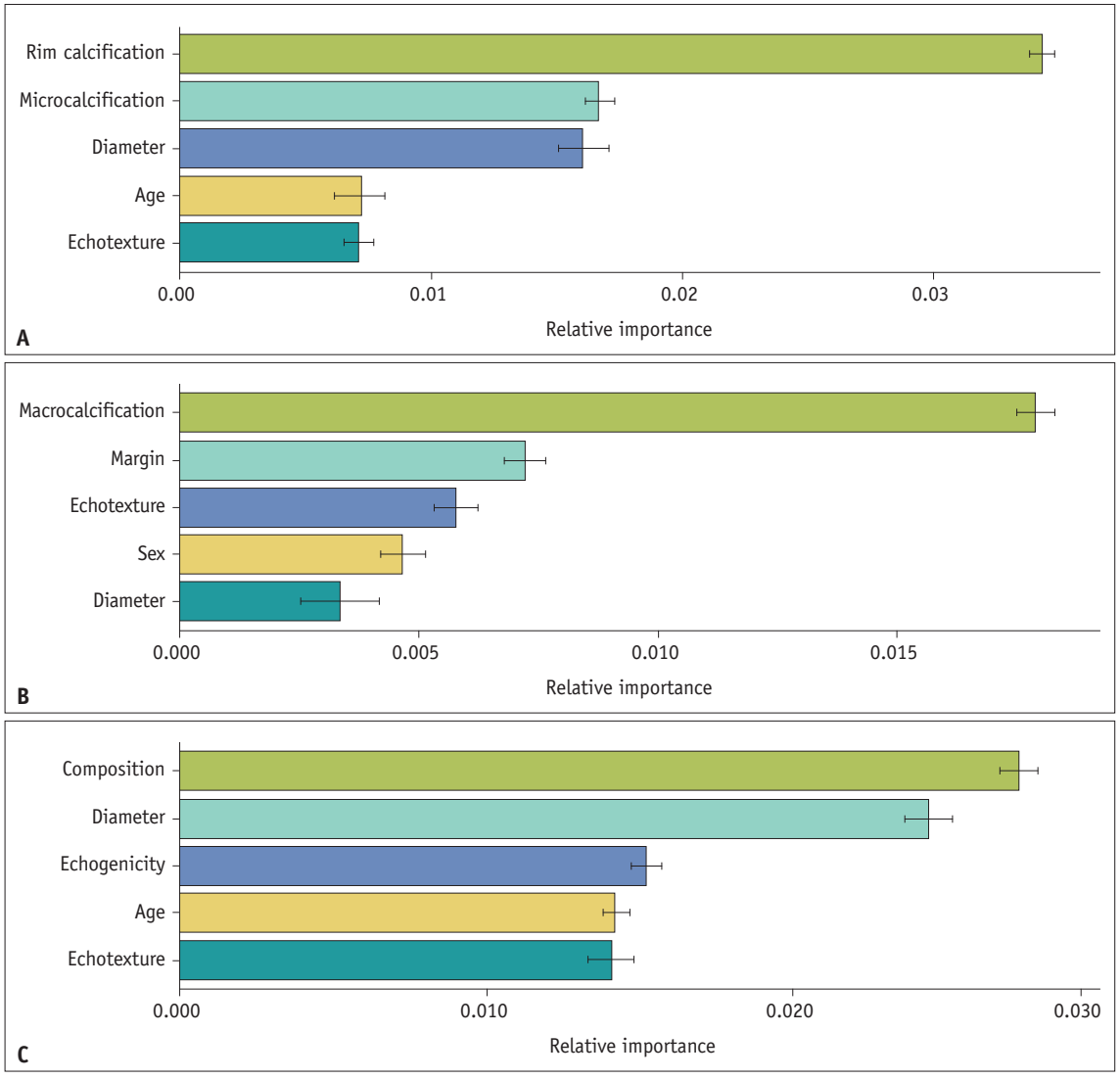

Fig. 2. The top five features important for distinguishing FC from FA (A), FVPTC from FA (B), and FC/FVPTC from BN/FA (C). BN = benign follicular nodule, FA = follicular adenoma, FC = follicular carcinoma, FVPTC = follicular variant of papillary thyroid carcinoma

echotexture were the top five variables for differentiating FC from FA, whereas macrocalcifications, non-smooth margin, mixed echotexture, sex, and maximal tumor diameter were the top five variables distinguishing FVPTC from FA. Solid composition, maximal tumor diameter, hypoechogenicity, age, and mixed echotexture were the top five variables for the differential diagnosis of BN/FA and follicular-patterned malignancies (FC and FVPTC).

DISCUSSION

Our multicenter cohort study showed that FA, FC, and FVPTC could be distinguished from BN based on their larger diameter, solid composition, hypoechogenicity, halo, and the younger age of patients associated with them. Compared to FA, FC tumors were of larger diameter and characterized by rim calcifications, whereas FVPTC had a smaller diameter and differed by their macrocalcifications, non-smooth margin, and younger age. Although follicular-patterned lesions have overlapping clinical, radiological, and cytological features, the relative importance of these features, as assessed in a large clinical cohort, may provide valuable information for preoperative decision-making.

The term "follicular" refers to either thyroid parenchymal cells or the growth pattern of a thyroid lesion, that is, follicle formation or follicular patterning [5,6]. Follicular-patterned lesions, including BNs, FAs, FCs, and FVPTCs, are commonly encountered in practice and are classified as benign or malignant based on the size of the follicles (microfollicular vs. macrofollicular) and the presence/

https://doi.org/10.3348/kjr.2022.0079

absence of nuclear features of papillary thyroid carcinoma, as determined by FNA [5,6]. However, preoperative differentiation of follicular-patterned lesions based on cytology alone remains challenging [4-6,8-12,21]. After FNA, nodules with cytological/architectural atypia are commonly assigned to the AUS/FLUS category [4]. Because the estimated risk of malignancy is 10%–30%, repetitive FNAs and diagnostic lobectomy are usually performed [1-4].

The radiological distinction of definite BN from a follicular-patterned neoplasm, whether FA, FC, or FVPTC, is important to prevent repetitive FNA and diagnostic surgery [6-9,11,22-24]. Tumor diameter, solid composition, hypoechogenicity, halo, and younger patient age were significant for differentiating BN from follicular-patterned neoplasms. Compared to the mean diameter of BN (20.8 ± 10.5 mm), those of FA (29.4 ± 14.9 mm), FC (34.5 ± 14.4 mm), and FVPTC (22.9 ± 12.9 mm) were significantly larger. More than half of the follicular-patterned tumors had a solid composition, particularly in FC (62.9%) and FVPTC (72.6%). Although follicular-patterned neoplasms in isoechoic nodules cannot be ruled out, in our cohort, hypoechogenicity occurred significantly more often in follicular-patterned neoplasms (39.0%–48.4%) than in BNs (27.6%). Previous studies have suggested that echogenicity may correlate with pathological growth patterns [8]. Thus, tumors with a solid/trabecular, macrofollicular, or microfollicular growth pattern tend to be markedly hypoechogenic or mildly hypoechogenic, and those with a normofollicular pattern tend to be isoechogenic [8]. Although follicular lesions of the thyroid can have similar architectural growth patterns, a normofollicular growth pattern is commonly seen in BNs, whereas microfollicular and solid/trabecular growth patterns are more frequently found in follicular-patterned neoplasms. In addition, the presence of tumor necrosis, hemorrhage, or both could also account for hypoechogenicity in follicular-patterned neoplasm [8]. The detection of a halo also distinguished FA, FC, and FVPTC from BN (OR 1.927 in our study). Histologically, the halo or hypoechoic rim surrounding a nodule comprises the nodule capsule or pseudocapsule of the surrounding capsular vessels, fibrous connective tissue, compressed thyroid parenchyma, and chronic inflammatory infiltrates [25-27]. In this study, the presence of a definite thin or thick halo in > 50% of the nodules accounted for the detection of a follicular-patterned neoplasm in 56.6%–59.7% of FA/FC and 49.2% of FVPTC. These findings are consistent with the emphasis on the importance of obtaining the nodule-parenchymal border from CNB in the differential diagnosis of follicular-patterned lesions [28].

The radiological distinction of FA from follicular-patterned malignancies, such as FC or FVPTC, can lead to active surveillance in selected patients [1]. Although diagnostic lobectomy is the usual management for these nodules, US follow-up instead of immediate surgery can be considered depending on the size, US features, and clinical status of the nodule, as well as patient preference, thus reducing the risk of overtreatment [1]. In this study, FC was distinguished from FA by the presence of rim calcification (17.7% vs. 2.2%; OR: 16.692). Although rim calcifications in a thyroid nodule are generally not associated with malignancy [29], they can be explained by calcifications occurring in the thickened and/or hyalinized capsule [8]. This result is similar to that of Shin et al. [29], who reported that the frequency of rim calcification was significantly higher in FCs than in papillary thyroid cancers (14.3% vs. 1.4%), and that the presence of rim calcification significantly increased the risk of FCs (5.3% vs. 0.7%) in all nodules. Conversely, FVPTC differed significantly from FA by the presence of macrocalcifications (20.3% vs. 6.6%) and non-smooth margins (19.5% vs. 6.6%). Macrocalcifications can be secondary to tissue necrosis, hemorrhage, or both (dystrophic calcifications) and, thus, more common in FVPTC than in FA.

This study has several clinical implications. First, the US features highly predictive of malignant nodules (microcalcification, nonparallel orientation, irregular margin) in the current risk stratification systems were less helpful in differentiating follicular-patterned malignancies (FC and FVPTC) from benign lesions (BN and/or FA). As the current risk stratification systems are mainly focused on the prediction of papillary thyroid carcinomas, they may not be accurate in the prediction of follicular-patterned neoplasms or malignancies. These results are consistent with those of Lin et al. [30] that the current US-based malignancy risk stratification systems for thyroid nodules had low efficiency in the characterization of follicular neoplasms. Therefore, a different classification system may be necessary to stratify patients with follicular-patterned lesions who may benefit from or who should have a pathologic diagnosis [30]. In this regard, we consider that the malignancy risk of nodules with macrocalcifications or rim calcifications may be reconsidered when detecting follicular-patterned malignancies. Second, we showed that the malignancy risk of follicular-patterned lesions which do not present features such as solid hypoechogenicity or any of calcifications was

https://doi.org/10.3348/kjr.2022.0079

Korean Journal of Radiology
KJR

1.5% (35/2385) in nodules < 3.0 cm, 1.7% (44/2621) in nodules < 3.5 cm, and 2.0% (55/2806) in nodules < 4.0 cm. These patients should be carefully monitored and spared from surgery. However, further large-scale studies are needed to confirm the findings of this study.

This study had several limitations, including its retrospective design and the fact that the US images were not interpreted by the same person who conducted the examination, which may have biased the results. Only surgical cases of FA, FC, and FVPTC were included, which may have led to a selection bias. Owing to the lower incidence of FTCs, the number of study patients with these nodules was relatively low, such that the clinical and sonographic features may not have been fully representative. Since most BNs are diagnosed based on FNA or CNB results, there may be false-negative results. However, considering that BNs generally do not undergo surgery, these criteria were applied to reduce selection bias and reflect clinical practice. Among the surgically confirmed BNs (n = 258), there were hyperplastic or adenomatoid nodules (n = 245), thyroiditis (n = 8), and others (n = 5), including degenerating nodules. In addition, a new classification, non-invasive follicular thyroid neoplasm with papillary-like nuclear features, could not be applied in this study because the nodules included in this study were retrospectively collected from June to September 2015. Therefore, they may be included in FVPTC. There may also be inter-observer variations in cytological diagnoses in each institution. Finally, the study did not include color Doppler findings because of the retrospective interpretation of images.

In conclusion, although follicular-patterned lesions have overlapping clinical and radiological features, the distinguishing features identified in our large clinical cohort may provide valuable information for preoperative distinction between them and decision-making regarding their management.

Supplement

The Supplement is available with this article at https://doi.org/10.3348/kjr.2022.0079.

Availability of Data and Material

The datasets generated or analyzed during the study are available from the corresponding author on reasonable request.

Conflicts of Interest

Ji-hoon Kim who is on the editorial board of the *Korean Journal of Radiology* was not involved in the editorial evaluation or decision to publish this article. All remaining authors have declared no conflicts of interest.

Author Contributions

Conceptualization: Eun Ju Ha. Data curation: Eun Ju Ha, Ji-hoon Kim. Formal analysis: Jeong Hoon Lee. Funding acquisition: Eun Ju Ha. Investigation: Eun Ju Ha, Ji-hoon Kim. Methodology: Eun Ju Ha, Jeong Hoon Lee. Supervision: Eun Ju Ha, Ji-hoon Kim. Validation: Miran Han, Jung Hyun Park, Da Hyun Lee. Writing—original draft: Eun Ju Ha, Jeong Hoon Lee. Writing—review & editing: Miran Han, Da Hyun Lee, Jung Hyun Park, Ji-hoon Kim.

ORCID iDs

Jeong Hoon Lee
https://orcid.org/0000-0002-1789-8270
Eun Ju Ha
https://orcid.org/0000-0002-1234-2919
Da Hyun Lee
https://orcid.org/0000-0001-7593-0403
Miran Han
https://orcid.org/0000-0001-7752-5858
Jung Hyun Park
https://orcid.org/0000-0001-8636-569X
Ji-hoon Kim
https://orcid.org/0000-0002-6349-6950

Funding Statement

This work was supported by the Korean Thyroid Association Clinical Research Award 2019.

REFERENCES

1. Ha EJ, Chung SR, Na DG, Ahn HS, Chung J, Lee JY, et al. 2021 Korean thyroid imaging reporting and data system and imaging-based management of thyroid nodules: Korean Society of Thyroid Radiology consensus statement and recommendations. *Korean J Radiol* 2021;22:2094-2123
2. Haugen BR, Alexander EK, Bible KC, Doherty GM, Mandel SJ, Nikiforov YE, et al. 2015 American Thyroid Association management guidelines for adult patients with thyroid nodules and differentiated thyroid cancer: the American Thyroid Association guidelines task force on thyroid nodules and differentiated thyroid cancer. *Thyroid* 2016;26:1-133
3. Tessler FN, Middleton WD, Grant EG, Hoang JK, Berland

LL, Teefey SA, et al. ACR thyroid imaging, reporting and data system (TI-RADS): white paper of the ACR TI-RADS Committee. *J Am Coll Radiol* 2017;14:587-595
4. Cibas ES, Ali SZ. The 2017 Bethesda system for reporting thyroid cytopathology. *Thyroid* 2017;27:1341-1346
5. Baloch ZW, LiVolsi VA. Our approach to follicular-patterned lesions of the thyroid. *J Clin Pathol* 2007;60:244-250
6. Jeong SH, Hong HS, Lee EH. Can nodular hyperplasia of the thyroid gland be differentiated from follicular adenoma and follicular carcinoma by ultrasonography? *Ultrasound Q* 2016;32:349-355
7. Sillery JC, Reading CC, Charboneau JW, Henrichsen TL, Hay ID, Mandrekar JN. Thyroid follicular carcinoma: sonographic features of 50 cases. *AJR Am J Roentgenol* 2010;194:44-54
8. Li W, Song Q, Lan Y, Li J, Zhang Y, Yan L, et al. The value of sonography in distinguishing follicular thyroid carcinoma from adenoma. *Cancer Manag Res* 2021;13:3991-4002
9. Kuo TC, Wu MH, Chen KY, Hsieh MS, Chen A, Chen CN. Ultrasonographic features for differentiating follicular thyroid carcinoma and follicular adenoma. *Asian J Surg* 2020;43:339-346
10. Park JW, Kim DW, Kim D, Baek JW, Lee YJ, Baek HJ. Korean thyroid imaging reporting and data system features of follicular thyroid adenoma and carcinoma: a single-center study. *Ultrasonography* 2017;36:349-354
11. Yoon RG, Baek JH, Lee JH, Choi YJ, Hong MJ, Song DE, et al. Diagnosis of thyroid follicular neoplasm: fine-needle aspiration versus core-needle biopsy. *Thyroid* 2014;24:1612-1617
12. Glass RE, Marotti JD, Kerr DA, Levy JJ, Vaickus LJ, Gutmann EJ, et al. Using molecular testing to improve the management of thyroid nodules with indeterminate cytology: an institutional experience with review of molecular alterations. *J Am Soc Cytopathol* 2022;11:79-86
13. Ha EJ, Shin JH, Na DG, Jung SL, Lee YH, Paik W, et al. Comparison of the diagnostic performance of the modified Korean thyroid imaging reporting and data system for thyroid malignancy with three international guidelines. *Ultrasonography* 2021;40:594-601
14. Chung SR, Ahn HS, Choi YJ, Lee JY, Yoo RE, Lee YJ, et al. Diagnostic performance of the modified Korean thyroid imaging reporting and data system for thyroid malignancy: a multicenter validation study. *Korean J Radiol* 2021;22:1579-1586
15. Tibshirani R. Regression shrinkage and selection via the lasso. *J R Stat Soc* 1996;58:267-288
16. Heinze G, Schemper M. A solution to the problem of separation in logistic regression. *Stat Med* 2002;21:2409-2419
17. Ishwaran H, Kogalur UB. Fast unified random forests for survival, regression, and classification (RF-SRC). R package version 2.12.1. cran.r-project.org Web site. https://cran.r-project.org/web/packages/randomForestSRC/index.html. Published 2019. Accessed January 3, 2022
18. Ishwaran H, O'Brien R. Commentary: the problem of class imbalance in biomedical data. *J Thorac Cardiovasc Surg* 2021;161:1940-1941
19. O'Brien R, Ishwaran H. A random forests quantile classifier for class imbalanced data. *Pattern Recognit* 2019;90:232-249
20. Kubat M, Holte R, Matwin S. *Learning when negative examples abound*. *European Conference on Machine Learning*. Berlin: Springer 1997
21. Shin I, Kim YJ, Han K, Lee E, Kim HJ, Shin JH, et al. Application of machine learning to ultrasound images to differentiate follicular neoplasms of the thyroid gland. *Ultrasonography* 2020;39:257-265
22. Hahn SY, Shin JH, Oh YL, Kim TH, Lim Y, Choi JS. Role of ultrasound in predicting tumor invasiveness in follicular variant of papillary thyroid carcinoma. *Thyroid* 2017;27:1177-1184
23. Jang EK, Kim WG, Choi YM, Jeon MJ, Kwon H, Baek JH, et al. Association between neck ultrasonographic findings and clinico-pathological features in the follicular variant of papillary thyroid carcinoma. *Clin Endocrinol (Oxf)* 2015;83:968-976
24. Rhee SJ, Hahn SY, Ko ES, Ryu JW, Ko EY, Shin JH. Follicular variant of papillary thyroid carcinoma: distinct biologic behavior based on ultrasonographic features. *Thyroid* 2014;24:683-688
25. Scheible W, Leopold GR, Woo VL, Gosink BB. High-resolution real-time ultrasonography of thyroid nodules. *Radiology* 1979;133:413-417
26. Propper RA, Skolnick ML, Weinstein BJ, Dekker A. The nonspecificity of the thyroid halo sign. *J Clin Ultrasound* 1980;8:129-132
27. Lu C, Chang TC, Hsiao YL, Kuo MS. Ultrasonographic findings of papillary thyroid carcinoma and their relation to pathologic changes. *J Formos Med Assoc* 1994;93:933-938
28. Na DG, Baek JH, Jung SL, Kim JH, Sung JY, Kim KS, et al. Core needle biopsy of the thyroid: 2016 consensus statement and recommendations from Korean Society of Thyroid Radiology. *Korean J Radiol* 2017;18:217-237
29. Shin HS, Na DG, Paik W, Yoon SJ, Gwon HY, Noh BJ, et al. Malignancy risk stratification of thyroid nodules with macrocalcification and rim calcification based on ultrasound patterns. *Korean J Radiol* 2021;22:663-671
30. Lin Y, Lai S, Wang P, Li J, Chen Z, Wang L, et al. Performance of current ultrasound-based malignancy risk stratification systems for thyroid nodules in patients with follicular neoplasms. *Eur Radiol* 2022;32:3617-3630

https://doi.org/10.3348/kjr.2022.0079